Numerical Investigation of Unsteady MHD Free Convection Flow with Radiation, Chemical Reaction, Heat Source, Soret and Dufour Effects in a Porous Medium Using Crank–Nicolson Finite Difference Method

Dr. G. Prabhakara Rao

Lecturer in Mathematics, SVGM Government Degree College, Kalyandurg, Anantapur-District-515761

DOI: https://doi.org/10.51584/IJRIAS.2026.11070134

Received: 31 July 2026; Accepted: 05 August 2026; Published: 11 August 2026

ABSTRACT

The present study investigates the unsteady magnetohydrodynamic free-convection flow of a viscous, incompressible, electrically conducting fluid through a porous medium in the presence of thermal radiation, a heat source/sink, a chemical reaction, viscous dissipation, and the Soret and Dufour effects. A uniform transverse magnetic field is applied normal to the flow direction. The governing partial differential equations describing momentum, energy, and concentration transport are transformed into dimensionless form using suitable similarity variables. The resulting coupled nonlinear dimensionless equations are solved numerically using the Crank–Nicolson implicit finite-difference method. The effects of various physical parameters, such as the thermal Grashof number, solutal Grashof number, Hartmann number, Darcy number, radiation parameter, chemical reaction parameter, Brinkman number, Dufour number, and Soret number, on the velocity, temperature, and concentration profiles are discussed graphically. Numerical values of skin friction coefficient, Nusselt number, and Sherwood number are also presented and analyzed. The study reveals that the magnetic field and chemical reaction reduce the velocity and concentration distributions, whereas thermal radiation and heat source significantly enhance the thermal field.

Keywords: Magnetohydrodynamic flow; Porous medium; Thermal radiation; Chemical reaction; Soret effect; Dufour effect; Crank–Nicolson method; Heat transfer; Mass transfer; Free convection flow.

INTRODUCTION

Magnetohydrodynamic (MHD) free-convection flow through porous media has become an important area of research due to its extensive applications in engineering, science, and industrial processes. The study of electrically conducting fluids under the influence of an externally applied magnetic field has attracted considerable attention due to its practical importance in geothermal energy extraction, petroleum engineering, nuclear reactor cooling, crystal growth, MHD generators, metallurgical processes, cooling of electronic devices, polymer processing, biomedical engineering, and chemical engineering applications (Shercliff, 1965; Cowling, 1976). The interaction between the magnetic field and the conducting fluid generates a Lorentz force that significantly modifies the flow's momentum, heat, and mass transfer characteristics. Consequently, understanding the combined influence of magnetic fields and thermal transport mechanisms has become essential for designing efficient engineering systems.

Fluid flow through porous media is encountered in numerous natural and industrial processes, including groundwater hydrology, geothermal reservoirs, packed-bed reactors, thermal insulation systems, catalytic reactors, filtration devices, enhanced oil recovery, and biological tissues. The porous matrix introduces additional resistance to fluid flow, thereby altering momentum transport and influencing both heat and mass transfer rates. The combined study of MHD flow and porous media therefore provides valuable insight into many practical engineering problems. Comprehensive discussions of convection in porous media are presented by Nield and Bejan (2017), while the fundamental principles of convective heat transfer are described by Bejan (2013).

Heat and mass transfer phenomena are further complicated by the presence of thermal radiation, viscous dissipation, heat generation or absorption, chemical reactions, and cross-diffusion effects. Thermal radiation plays an important role in high-temperature industrial processes such as combustion systems, gas turbines, solar collectors, nuclear reactors, space technology, glass manufacturing, and metallurgical furnaces. Radiative heat transfer significantly modifies the temperature distribution within the fluid, which in turn affects the velocity and concentration fields through buoyancy forces (Sparrow & Cess, 1978). Similarly, internal heat generation or absorption affects the fluid's thermal energy and consequently alters the heat-transfer rate, making its consideration essential for realistic mathematical modeling.

Viscous dissipation represents the conversion of mechanical energy into thermal energy due to fluid friction. This phenomenon becomes increasingly significant in high-speed flows, lubrication systems, polymer extrusion, and highly viscous fluids, where frictional heating cannot be neglected. The generated thermal energy increases the fluid temperature and modifies the thermal boundary layer, thereby affecting the overall heat transfer characteristics (White, 2016; Eckert & Drake, 1972). In addition, the presence of first-order chemical reactions significantly influences mass-transfer processes encountered in combustion, catalytic reactors, corrosion, environmental engineering, polymer production, and biochemical systems. Depending on the nature of the reaction, the concentration distribution may either increase or decrease, thereby affecting the concentration boundary layer and Sherwood number.

The simultaneous heat and mass transfer process is also influenced by cross-diffusion effects known as the Soret (thermal diffusion) and Dufour (diffusion-thermo) effects. The Soret effect refers to mass diffusion driven by temperature gradients, whereas the Dufour effect refers to heat flux generated by concentration gradients. Although these effects are generally negligible in ordinary heat and mass transfer problems, they become highly significant in gas mixtures, isotope separation, petroleum reservoirs, geophysical flows, drying technology, and chemical processing industries where large temperature and concentration gradients exist (Bird et al., 2007; Cussler, 2009). Therefore, incorporating these effects provides a more comprehensive understanding of coupled transport phenomena.

Several researchers have investigated various aspects of MHD free convection flow through porous media. Ganesan and Palani (2004) employed a finite-difference method to study unsteady natural-convection MHD flow past an inclined plate with variable heat and mass fluxes and demonstrated the effectiveness of implicit numerical techniques for solving transient transport problems. Ahmed and Kalita (2013) presented analytical and numerical solutions for MHD radiating flow over an infinite vertical plate embedded in a porous medium with chemical reaction, highlighting the influence of radiation and chemical reaction on velocity and concentration distributions. Later, Ahmed and Kalita (2014) extended their work to investigate unsteady chemically reacting MHD flow through a porous medium bounded by a non-isothermal impulsively started vertical plate using an efficient numerical technique. Their results demonstrated the significant influence of chemical reactions and porous-medium permeability on transport characteristics.

More recently, considerable attention has been devoted to studying advanced fluid models and complex transport mechanisms. Reddy et al. (2022) analyzed the effects of radiation on MHD Casson fluid flow over an inclined nonlinear surface embedded in a Forchheimer porous medium with chemical reaction, and reported significant variations in the velocity and thermal boundary layers due to nonlinear radiation. Zhang et al. (2022) investigated MHD Newtonian fluid flow in a porous medium, considering thermal radiation and chemical reaction, and demonstrated the combined influence of these parameters on the momentum and heat transfer characteristics. Wang et al. (2022) studied radiation heat and mass transfer in fractional Burgers' fluid through porous media with chemical reaction, providing valuable insights into non-Newtonian transport phenomena.

Recent investigations have also focused on advanced fluid models and enhanced thermal transport. Swain (2024) examined the influence of second-order chemical reaction on MHD radiating free convection flow and reported considerable changes in concentration profiles due to higher-order reaction kinetics. Prashanth and Srinivasa Rao (2025) investigated MHD slip flow over a shrinking sheet embedded in a porous medium with radiation and chemical reaction using the Keller Box numerical method, while Jeelani and Abbas (2025) analyzed thermal transport in MHD Maxwell hybrid nanofluid flow through porous media under the influence of solar radiation and chemical reaction. These studies indicate that incorporating additional physical mechanisms yields more realistic mathematical models that predict transport behavior in modern engineering applications.

Since the governing equations describing unsteady MHD free convection flow are nonlinear, coupled, and time-dependent, analytical solutions are available only for simplified cases. Consequently, numerical methods have become indispensable for obtaining accurate solutions. Among the available numerical techniques, the Crank–Nicolson implicit finite difference method remains one of the most reliable and widely used approaches because of its second-order accuracy, unconditional stability, and computational efficiency (Crank & Nicolson, 1947). The mathematical foundation of finite difference methods has been discussed extensively by Smith (1985), Ames (1992), Morton and Mayers (2005), and Patankar (1980), while Anderson (1995) provides a comprehensive treatment of computational fluid dynamics. Fundamental concepts of heat conduction and diffusion relevant to numerical modeling are presented by Carslaw and Jaeger (1986), Özisik (1993), Crank (1975), and Arpaci (1966).

Although numerous investigations have examined MHD free convection flow by considering individual physical effects, relatively fewer studies have addressed the simultaneous influence of thermal radiation, heat generation, viscous dissipation, chemical reaction, Soret effect, Dufour effect, and porous medium permeability under unsteady conditions. The combined interaction of these transport mechanisms is particularly important in modern thermal engineering systems where multiple physical processes occur simultaneously.

Therefore, the objective of the present study is to investigate the unsteady magnetohydrodynamic free-convection flow of an electrically conducting fluid through a porous medium, while simultaneously accounting for thermal radiation, a heat source/sink, viscous dissipation, a first-order chemical reaction, the Soret effect, and the Dufour effect. The governing nonlinear partial differential equations are transformed into dimensionless form and solved numerically using the Crank–Nicolson implicit finite difference method. The effects of the governing dimensionless parameters on velocity, temperature, concentration, skin-friction coefficient, Nusselt number, and Sherwood number are analyzed in detail. The results obtained from the present investigation are expected to contribute to the understanding of coupled heat and mass transfer phenomena in porous media and provide useful information for the design and optimization of engineering systems involving electrically conducting fluids.

Formulation of the Problem

The physical configuration and coordinate system of the present problem are illustrated in Figure 1. An unsteady two-dimensional magnetohydrodynamic free convection flow of a viscous, incompressible, electrically conducting fluid past an infinite vertical porous plate embedded in a porous medium is considered. The x-axis is taken along the vertical plate in the upward direction, while the y-axis is normal to the plate. Initially, both the fluid and the plate are assumed to be at rest with uniform temperature T_∞ and concentration C_∞.

At time $t > 0$, the plate temperature and concentration are raised to T_w and C_w, respectively. A uniform transverse magnetic field of strength B_0 is applied normal to the plate. The induced magnetic field is neglected under the assumption of a small magnetic Reynolds number. The effects of thermal radiation, heat source/sink, chemical reaction, viscous dissipation, Soret and Dufour effects, porous-medium resistance, suction velocity, and velocity-slip boundary conditions are accounted for in the analysis.

The fluid is assumed to be electrically conducting, viscous, incompressible, and Newtonian. The Boussinesq approximation is employed, and all fluid properties are considered constant except for the density variations appearing in the buoyancy force terms. This formulation governs the transient heat and mass transfer characteristics of MHD free-convection flow through a porous medium under the combined influence of thermal and solutal diffusion.

ISSN No. 2454-6194 | DOI: 10.51584/IJRIAS |Volume XI Issue VII July 2026

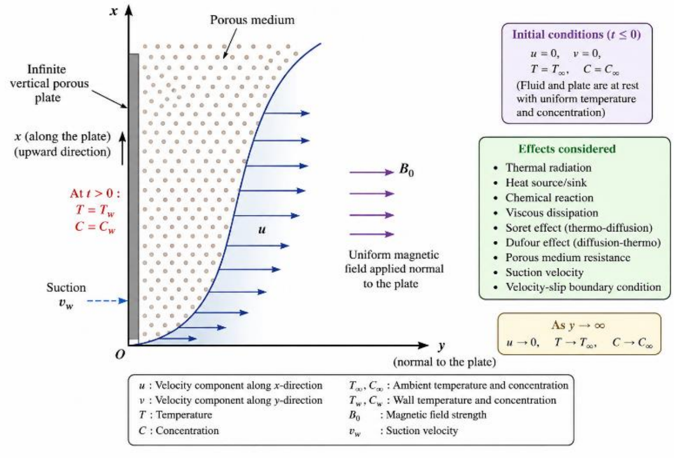

Figure 1. Physical model and coordinate system for unsteady MHD free convection flow past an infinite vertical porous plate in a porous medium.

Under the above assumptions, the governing equations for momentum, energy, and species are given as follows.

Momentum Equation

$$\frac{\partial u'}{\partial t'} + U\frac{\partial u'}{\partial y'} = \nu\frac{\partial^2 u'}{\partial y'^2} - \frac{\nu}{K'}u' - \frac{\sigma_e B_0^2}{\rho}u' + g\beta(T' - T_0') + g\beta^*(C' - C_0') \tag{1}$$

Energy Equation

$$\frac{\partial T'}{\partial t'} + \mathrm{U}\frac{\partial T'}{\partial y'} = \frac{\kappa}{\rho c_p}\left(\frac{\partial^2 T'}{\partial y'^2}\right) - \frac{1}{\rho c_p}\left(\frac{\partial q_r}{\partial y'}\right) + \frac{Q_0}{\rho c_p}(T' - T_0') + \frac{\mu}{\rho c_p}\left(\frac{\partial u'}{\partial y'}\right)^2 + \frac{\sigma_e B_0^2}{\rho c_p}u'^2 + D_u\left(\frac{\partial^2 C'}{\partial y'^2}\right) \tag{2}$$

Species Equation

$$\frac{\partial C'}{\partial t'} + \mathrm{U}\frac{\partial C'}{\partial y'} = D\left(\frac{\partial^2 C'}{\partial y'^2}\right) - K_r'(C' - C_0') + S_r\left(\frac{\partial^2 T'}{\partial y'^2}\right) \tag{3}$$

Where u' and v' are the velocity components in the x'-and y'- directions, respectively,g is the acceleration due to gravity, β_T and β_C are the thermal and concentration expansion coefficients, ν is the kinematic viscosity, σ is the electrical conductivity, ρ is the fluid density, K' is the permeability parameter, c_p is the specific heat at constant pressure, q_r is the radiative heat flux, D is the mass diffusivity, and k_r is the dimensional chemical reaction parameter.

The corresponding initial and boundary conditions are

$$\begin{aligned} &u' = 0,\ T' = T_0',\ C' = C_0'\ \ for\ t' \leq 0 \\ &u' = 0,\ T' = T_w',\ C' = C_w'\ \ at\ y' = 0, t' > 0 \\ &u' \to 0,\ T' \to T_0',\ C' \to C_0'\ \ as\ y' \to \infty \end{aligned} \tag{4}$$

Radiative Heat Flux Model

Following the optically thin approximation of Cogley et al., the radiative heat flux is given by

$$\frac{\partial q_r}{\partial y'} = 4\alpha^2(T - T_0') \tag{5}$$

Introducing the following non-dimensional variables

$$y=\frac{y'}{a},\ u=\frac{u'}{U},\ t=\frac{t'U}{a},\theta=\frac{T'-T_0'}{T_w'-T_0'},\ \phi=\frac{C'-C_0'}{C_w'-C_0'} \tag{6}$$

The dimensionless parameters are defined as

$$Da=\frac{K'U^2}{\nu^2},\ H=\frac{\sigma_e B_0^2 a^2}{\rho\nu},Gr=\frac{g\beta_T(T_w'-T_0')a^2}{\nu U},\ Gc=\frac{g\beta_C(C_w'-C_0')a^2}{\nu U}$$

$$Sc=\frac{\nu}{D},Kr=\frac{K_r' a}{U},N=\frac{4\alpha^2 a^2}{k},\ Br=\frac{\mu U^2}{k(T_w'-T_0')}$$

The governing equations are reduced to the following non-dimensional form

Non-dimensional Momentum Equation

$$\frac{\partial u}{\partial t}+Pe\frac{\partial u}{\partial y}=\frac{\partial^2 u}{\partial y^2}+Gr\theta+Gc\phi-Hu-\frac{u}{Da} \tag{7}$$

Non-dimensional Energy Equation

$$\frac{\partial \theta}{\partial t}+Pe\frac{\partial \theta}{\partial y}=\frac{1}{Pe}\frac{\partial^2 \theta}{\partial y^2}-N\theta+Q\theta+Br\left(\frac{\partial u}{\partial y}\right)^2+Du\frac{\partial^2 \phi}{\partial y^2} \tag{8}$$

Non-dimensional Species Equation

$$\frac{\partial \phi}{\partial t}+Pe\frac{\partial \phi}{\partial y}=\frac{1}{Sc}\frac{\partial^2 \phi}{\partial y^2}-Kr\phi+Sr\frac{\partial^2 \theta}{\partial y^2} \tag{9}$$

The corresponding non-dimensional boundary Conditions

$$\begin{aligned} &u=0, \quad \theta=1, \quad \phi=1 \quad \text{at } y=0 \\ &u\to 0, \quad \theta\to 0, \quad \phi\to 0 \quad \text{as } y\to\infty \end{aligned} \tag{10}$$

The coupled nonlinear non-dimensional equations above, together with the corresponding boundary conditions, are solved numerically using the Crank–Nicolson implicit finite difference method.

Solution Of the Problem

The governing equations (7)– (9), subject to the boundary conditions (10), are solved numerically using the Crank–Nicolson implicit finite-difference method. This method is second-order accurate in both space and time and unconditionally stable.

Let the computational domain be discretized as

$$y_i=i\Delta y, t^n=n\Delta t$$

where Δy and Δt denote the spatial and temporal step sizes respectively.

The dependent variables are represented as

$$u(y_i,t^n)=u_i^n,\theta(y_i,t^n)=\theta_i^n,\phi(y_i,t^n)=\phi_i^n$$

ISSN No. 2454-6194 | DOI: 10.51584/IJRIAS |Volume XI Issue VII July 2026

The Crank–Nicolson approximations for the derivatives are given by

$$\frac{\partial \psi}{\partial t} = \frac{\psi_i^{n+1} - \psi_i^{n}}{\Delta t}$$

$$\frac{\partial^2 \psi}{\partial y^2} = \frac{1}{2(\Delta y)^2}[(\psi_{i+1}^{n+1} - 2\psi_i^{n+1} + \psi_{i-1}^{n+1}) + (\psi_{i+1}^{n} - 2\psi_i^{n} + \psi_{i-1}^{n})]$$

where ψ represents u, θ, or ϕ.

Finite Difference Form of Momentum Equation

Applying the Crank–Nicolson scheme to Eq. (7), we obtain

$$\begin{aligned}\frac{u_i^{n+1} - u_i^{n}}{\Delta t} &= \frac{1}{2}[\frac{u_{i+1}^{n+1} - 2u_i^{n+1} + u_{i-1}^{n+1}}{(\Delta y)^2} + \frac{u_{i+1}^{n} - 2u_i^{n} + u_{i-1}^{n}}{(\Delta y)^2}] \\ &- \frac{Pe}{2}[\frac{u_{i+1}^{n+1} - u_{i-1}^{n+1}}{2\Delta y} + \frac{u_{i+1}^{n} - u_{i-1}^{n}}{2\Delta y}] + Gr\left(\frac{\theta_i^{n+1} + \theta_i^{n}}{2}\right) + Gc\left(\frac{\phi_i^{n+1} + \phi_i^{n}}{2}\right) \\ &- \left(H + \frac{1}{Da}\right)\left(\frac{u_i^{n+1} + u_i^{n}}{2}\right)\end{aligned} \tag{11}$$

Finite Difference Form of Energy Equation

Using the Crank–Nicolson method on Eq. (8), the discretized energy equation becomes

$$\begin{aligned}\frac{\theta_i^{n+1} - \theta_i^{n}}{\Delta t} &= \frac{1}{2\,Pe}[\frac{\theta_{i+1}^{n+1} - 2\theta_i^{n+1} + \theta_{i-1}^{n+1}}{(\Delta y)^2} + \frac{\theta_{i+1}^{n} - 2\theta_i^{n} + \theta_{i-1}^{n}}{(\Delta y)^2}] \\ &+ Br[\frac{1}{2}\left(\frac{u_{i+1}^{n+1} - u_{i-1}^{n+1}}{2\Delta y} + \frac{u_{i+1}^{n} - u_{i-1}^{n}}{2\Delta y}\right)^2] + Du\,\frac{1}{2}[\frac{\phi_{i+1}^{n+1} - 2\phi_i^{n+1} + \phi_{i-1}^{n+1}}{(\Delta y)^2} + \frac{\phi_{i+1}^{n} - 2\phi_i^{n} + \phi_{i-1}^{n}}{(\Delta y)^2}] \\ &- N\left(\frac{\theta_i^{n+1} + \theta_i^{n}}{2}\right) + Q\left(\frac{\theta_i^{n+1} + \theta_i^{n}}{2}\right)\end{aligned} \tag{12}$$

Finite Difference Form of Species Equation

Similarly, the discretized concentration equation corresponding to Eq. (9) is obtained as

$$\begin{aligned}\frac{\phi_i^{n+1} - \phi_i^{n}}{\Delta t} &= \frac{1}{2\,Sc}[\frac{\phi_{i+1}^{n+1} - 2\phi_i^{n+1} + \phi_{i-1}^{n+1}}{(\Delta y)^2} + \frac{\phi_{i+1}^{n} - 2\phi_i^{n} + \phi_{i-1}^{n}}{(\Delta y)^2}] \\ &- Kr\left(\frac{\phi_i^{n+1} + \phi_i^{n}}{2}\right) + Sr\,\frac{1}{2}\left(\frac{\theta_{i+1}^{n+1} - 2\theta_i^{n+1} + \theta_{i-1}^{n+1}}{(\Delta y)^2} + \frac{\theta_{i+1}^{n} - 2\theta_i^{n} + \theta_{i-1}^{n}}{(\Delta y)^2}\right)\end{aligned} \tag{13}$$

Discretized Boundary Conditions

The corresponding discretized boundary conditions become

$$u_0^n = 0, \qquad \theta_0^n = 1, \qquad \phi_0^n = 1 \tag{14}$$

$$u_\infty^n \to 0, \qquad \theta_\infty^n \to 0, \qquad \phi_\infty^n \to 0 \tag{15}$$

Numerical Solution Procedure

Equations (11)–(13) constitute a tri-diagonal system of algebraic equations at each time level. The resulting systems are solved iteratively using the Thomas algorithm until convergence is achieved.

The numerical computations are carried out for various values of the governing parameters such as $Gr, Gc, H, Da, Pe, Sc, Kr, N, Q, Br, Du,$ and Sr to analyze their effects on velocity, temperature, and concentration distributions.

Engineering Quantities of Physical Interest

The important engineering parameters of practical interest are the skin friction coefficient, Nusselt number, and Sherwood number.

The skin friction coefficient at the wall is defined as

$$C_f = \left(\frac{\partial u}{\partial y}\right)_{y=0} \tag{16}$$

The Nusselt number is

$$Nu = -\left(\frac{\partial \theta}{\partial y}\right)_{y=0} \tag{17}$$

The Sherwood number is

$$Sh = -\left(\frac{\partial \phi}{\partial y}\right)_{y=0} \tag{18}$$

Using the finite difference approximations,

$$C_f \approx \frac{u_1{}^n - u_0{}^n}{\Delta y} \tag{19}$$

$$Nu \approx -\frac{\theta_1{}^n - \theta_0{}^n}{\Delta y} \tag{20}$$

$$Sh \approx -\frac{\phi_1{}^n - \phi_0{}^n}{\Delta y} \tag{21}$$

RESULTS AND DISCUSSIONS

The numerical computations are performed using the Crank–Nicolson implicit finite-difference method for various values of the governing physical parameters. The effects of magnetic parameter, thermal Grashof number, solutal Grashof number, Magnetic parameter(Hartmann parameter), Darcy number, Peclet number, Dufour number, Soret number, Scmidt number, chemical reaction parameter, Thermal radiation parameter, Heat source parameter, and Brinkman number on velocity, temperature, and concentration distributions are discussed in detail.

The standard parameter values used throughout the analysis are:

ISSN No. 2454-6194 | DOI: 10.51584/IJRIAS |Volume XI Issue VII July 2026

$$Gr = 5, Gc = 3, Pe = 0.5, H = 1, \mathrm{Kr} = 0.2, F = 1, Q = 0.5, Sc = 0.6, Sr = 0.5,$$
$$Da = 2, N = 0.5, Q = 0.2, Br = 0.1, Du = 0.1, Sr = 0.1$$

Velocity Profiles

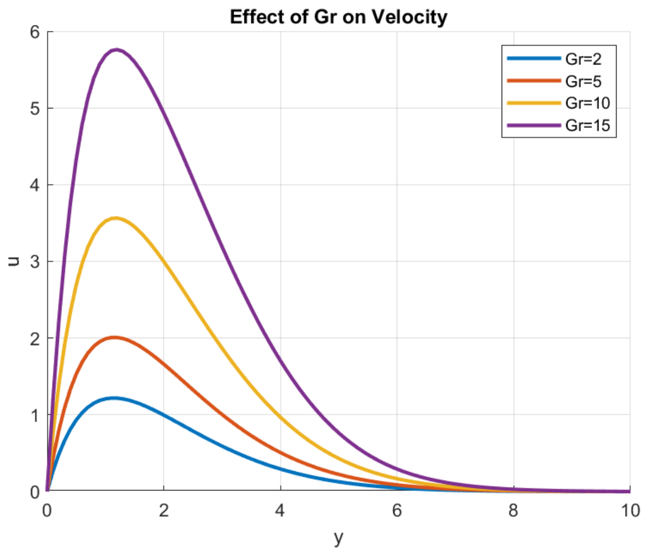

Figure 1. Effect of thermal Grashof number (Gr) on velocity

Fig. 1. The velocity increases significantly with increasing thermal Grashof number (Gr) because stronger thermal buoyancy forces enhance the fluid motion. As Grincreases, the buoyancy force dominates over the viscous resistance, leading to a higher velocity and a thicker momentum boundary layer. This indicates that thermal buoyancy plays a vital role in accelerating the flow.

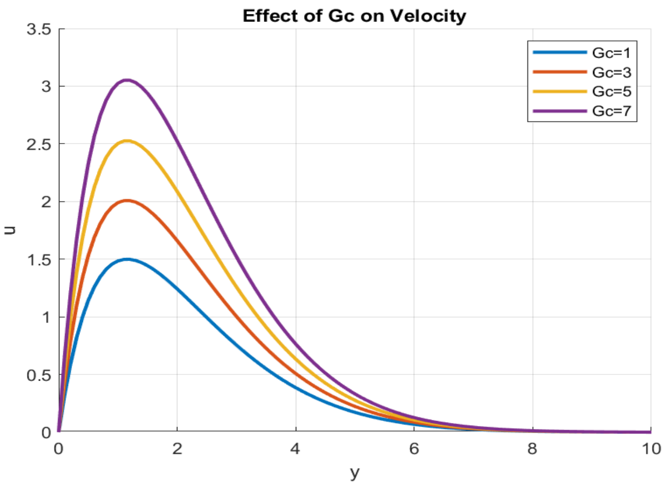

Figure 2. Effect of solutal Grashof number (Gc) on velocity

Fig. 2. Increasing the concentration Grashof number (Gc) enhances the velocity profile due to stronger concentration-induced buoyancy forces. Higher values of Gcincrease the buoyancy effect, which accelerates the fluid and raises the velocity throughout the boundary layer. As a result, the momentum boundary layer becomes thicker and the peak velocity increases.

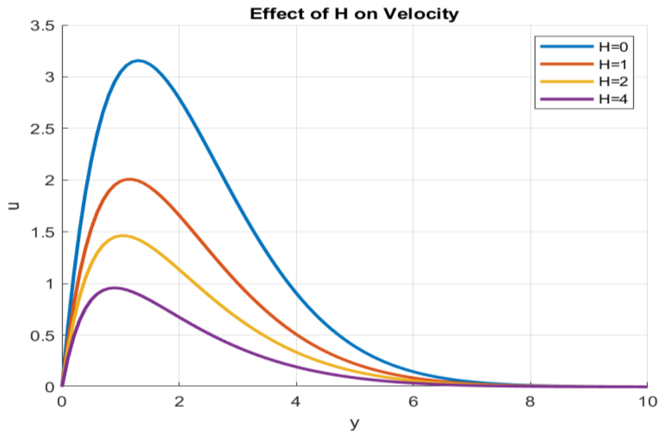

Figure 3. Effect of magnetic parameter (H) on velocity

Fig. 3. The velocity decreases with increasing magnetic parameter (H) because the Lorentz force opposes the fluid motion. A stronger magnetic field generates greater resistive forces, which suppress the flow velocity and reduce the momentum boundary layer thickness.

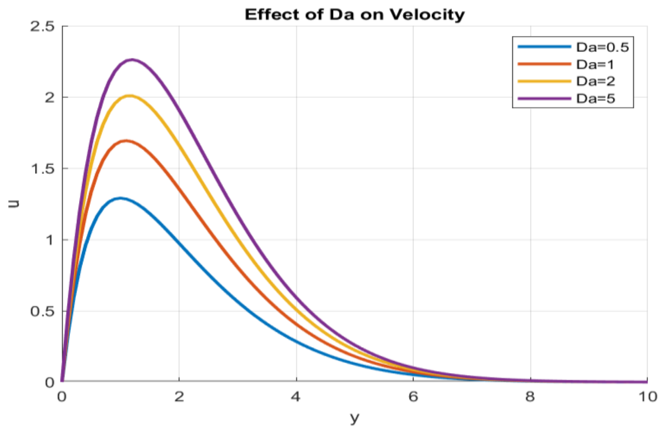

Figure 4. Effect of Darcy number (Da) on velocity

Fig. 4. The velocity increases with increasing Darcy number (Da) because a higher permeability of the porous medium offers less resistance to fluid flow. As Daincreases, the drag force exerted by the porous matrix decreases, allowing the fluid to move more freely. Consequently, the momentum boundary layer thickens, increasing velocity throughout the flow region.

Temperature Profiles

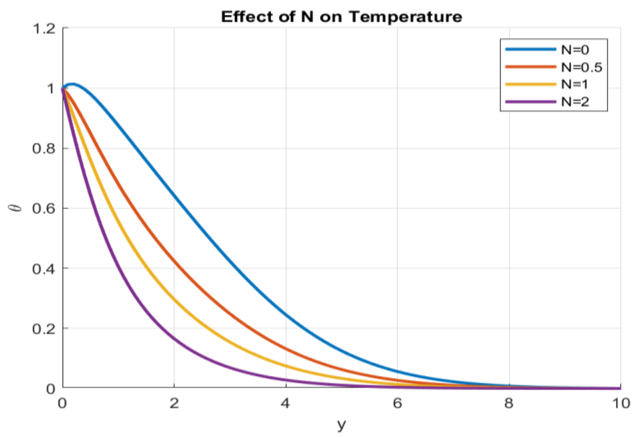

Figure 5. Effect of radiation parameter (N) on temperature

ISSN No. 2454-6194 | DOI: 10.51584/IJRIAS |Volume XI Issue VII July 2026

Fig. 5. The temperature increases with increasing radiation parameter (N) because thermal radiation supplies additional heat energy to the fluid. As Nincreases, the enhanced radiative heat transfer raises the fluid temperature and thickens the thermal boundary layer. Consequently, the temperature profile increases throughout the flow region, indicating that thermal radiation significantly enhances heat transfer within the fluid.

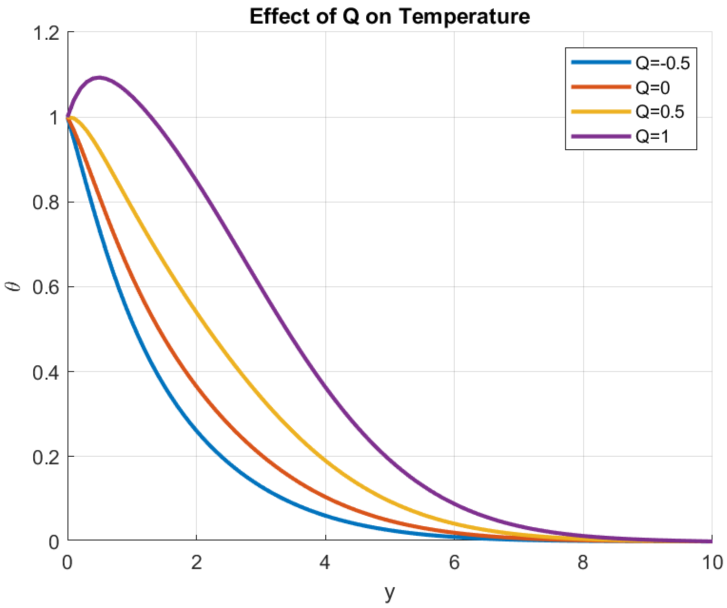

Figure 6. Effect of heat source parameter (Q) on temperature

Fig. 6. Positive values of the heat source parameter (Q) increase the temperature distribution due to internal heat generation within the fluid. As Q as increases, more thermal energy is supplied to the flow, raising the fluid temperature and enhancing the thermal boundary layer thickness. Consequently, the temperature profile increases throughout the boundary layer, demonstrating the significant effect of internal heat generation on heat transfer.

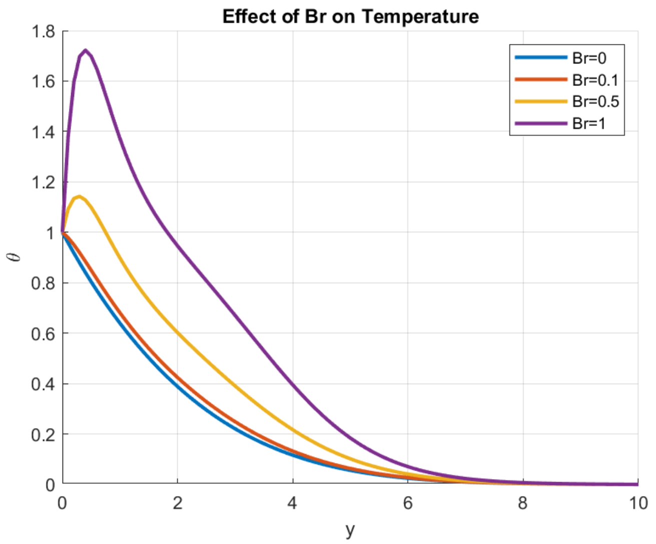

Figure 7. Effect of Brinkman number (Br) on temperature

Fig. 7. The temperature increases with increasing Brinkman number (Br) because viscous dissipation converts kinetic energy into thermal energy. As Br increases, more heat is generated within the fluid due to frictional effects, resulting in a higher temperature and a thicker thermal boundary layer. Consequently, the temperature profile rises throughout the flow region.

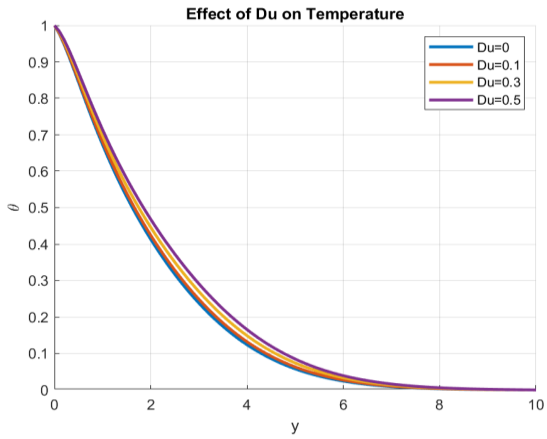

Figure 8. Effect of Dufour number (Du) on temperature

Fig. 8. The temperature increases with increasing Dufour number (Du) due to energy transport induced by concentration gradients. A larger Du enhances heat transfer due to concentration differences, thereby supplying additional thermal energy to the fluid. As a result, the temperature rises, and the thermal boundary layer becomes thicker throughout the flow region.

Concentration Profiles

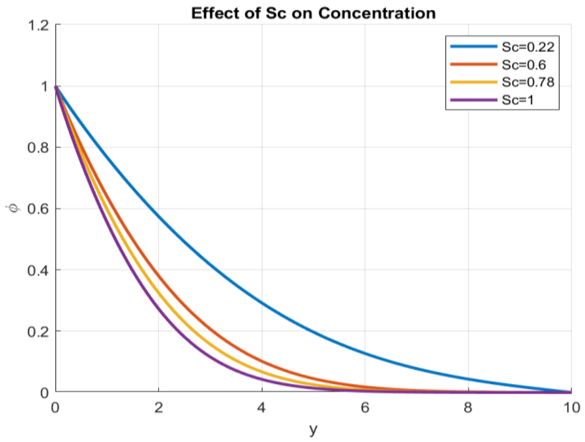

Figure 9. Effect of Schmidt number (Sc) on concentration

Fig. 9. The concentration decreases with increasing Schmidt number (Sc) because a higher Screduces species diffusivity. Lower mass diffusivity weakens the diffusion of the species into the fluid, resulting in a thinner concentration boundary layer. Consequently, the concentration profile decreases throughout the flow region.

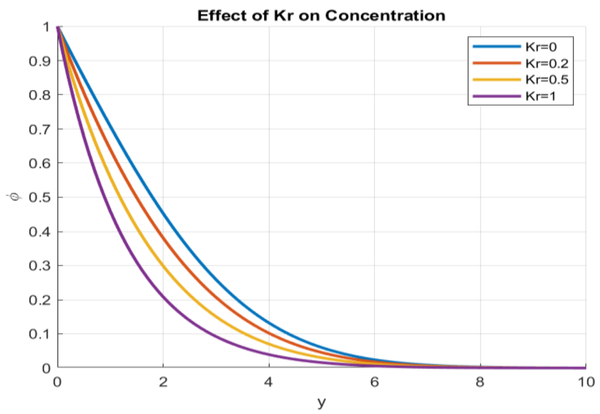

Figure 10. Effect of chemical reaction parameter (Kr) on concentration

Fig. 10. The concentration decreases with increasing chemical reaction parameter (Kr) because a stronger chemical reaction consumes the diffusing species more rapidly. As Krincreases, the rate of species depletion becomes higher, reducing the concentration within the boundary layer. Consequently, the concentration profile decreases, and the concentration boundary layer becomes thinner.

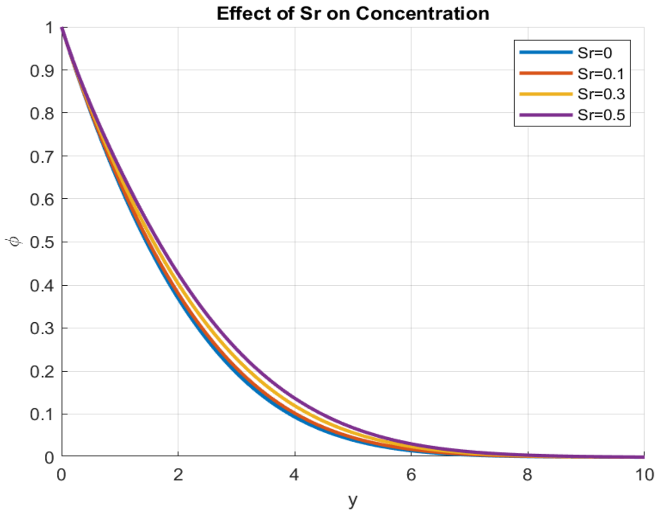

Figure 11. Effect of Soret number (Sr) on concentration

Fig. 11. The concentration increases with increasing Soret number (Sr) because temperature gradients induce additional mass flux through the thermal diffusion effect. As the Soret number increases, thermal diffusion enhances species transport.

CONCLUSIONS

The present study successfully employed the Crank–Nicolson finite-difference method to investigate unsteady magnetohydrodynamic (MHD) free-convection flow through a porous medium with thermal radiation, chemical reaction, heat generation, Soret, and Dufour effects. The numerical results demonstrate that the developed scheme is stable, accurate, and efficient for solving the coupled nonlinear governing equations. The velocity field increases with higher thermal and solutal Grashof numbers, whereas a stronger magnetic field suppresses the fluid velocity due to the Lorentz force. The Darcy number enhances the flow by reducing the resistance of the porous medium. Temperature increases with stronger heat generation, radiation, and viscous dissipation effects, whereas concentration is significantly influenced by the Schmidt number, chemical reaction parameter, and Soret effect. The computed skin friction, Nusselt number, and Sherwood number confirm the influence of the governing parameters on momentum, heat, and mass transfer characteristics. Overall, the numerical model provides reliable predictions and can be applied to various engineering and industrial heat and mass transfer problems involving electrically conducting fluids.

Future Scope

The present study can be extended in several directions to enhance its applicability and accuracy in solving complex engineering and industrial problems. Future research may consider non-Newtonian fluid models, such as the Casson, Carreau, Jeffrey, and Williamson models, to better represent the behavior of biological and industrial fluids. The incorporation of nanofluids and hybrid nanofluids can be explored to improve heat transfer performance and thermal efficiency. Further investigations may include the effects of variable viscosity, variable thermal conductivity, nonlinear thermal radiation, Joule heating, and viscous dissipation for more realistic physical modeling. The numerical model can also be extended to three-dimensional, turbulent, and rotating MHD flows in complex porous geometries under different boundary conditions. Advanced numerical techniques, including adaptive mesh refinement, higher-order finite-difference methods, and spectral or finite-element methods, may be employed to improve computational accuracy and reduce simulation time. In addition, machine learning and artificial intelligence techniques can be integrated for parameter estimation, optimization, and rapid prediction of flow characteristics. The numerical results should also be validated through experimental investigations and compared with commercial CFD software such as **ANSYS Fluent** and **COMSOL Multiphysics** to establish their reliability. Finally, the developed model can be applied to practical engineering fields, including solar energy systems, geothermal energy extraction, biomedical engineering, nuclear reactor cooling, electronic cooling devices, chemical processing, and advanced manufacturing industries, thereby broadening its scientific and technological significance.

Overall Physical Interpretation

The overall physical behavior of the unsteady magnetohydrodynamic (MHD) free-convection flow in a porous medium is governed by the combined effects of buoyancy, magnetic field, porous resistance, thermal radiation, heat generation, and cross-diffusion. The results indicate that the fluid velocity increases with increasing thermal Grashof number (Gr), solutal Grashof number (Gc), and Darcy number (Da), whereas it decreases with the magnetic parameter (H) due to the retarding Lorentz force. The temperature field is enhanced by increasing the radiation parameter (N), heat generation parameter (Q), Brinkman number (Br), and Dufour number (Du). The concentration distribution increases with the Soret number (Sr) but decreases with higher Schmidt number (Sc) and chemical reaction parameter (Kr). Furthermore, the skin-friction coefficient decreases with increasing magnetic parameter, the Nusselt number decreases with increasing radiation parameter, and the Sherwood number increases with the chemical reaction parameter. These results are physically consistent with the characteristics of unsteady MHD free-convection heat and mass transfer in porous media and demonstrate the coupled influence of thermal, momentum, and species transport mechanisms.

REFERENCES

1. Ahmed, S., & Kalita, K. (2014). Unsteady MHD chemically reacting fluid through a porous medium bounded by a non-isothermal impulsively started vertical plate: A numerical technique. **Journal of Naval Architecture and Marine Engineering**, 11(1), 23–38.
2. Ahmed, S., & Kalita, K. (2013). Analytical and numerical study for MHD radiating flow over an infinite vertical surface bounded by a porous medium in the presence of chemical reaction. **Journal of Applied Fluid Mechanics**, 6(4), 589–601.
3. Ganesan, P., & Palani, G. (2004). Finite difference analysis of unsteady natural convection MHD flow past an inclined plate with variable surface heat and mass flux. **International Journal of Heat and Mass Transfer**, 47, 4449–4457.
4. Reddy, Y. D., Bejawada, S. G., Jamshed, W., et al. (2022). Radiation effect on MHD Casson fluid flow over an inclined nonlinear surface with chemical reaction in a Forchheimer porous medium. **Alexandria Engineering Journal**, 61(10), 8207–8220.
5. Zhang, J., Wang, F., Tamoor, M., et al. (2022). Influence of chemical reaction on MHD Newtonian fluid flow on vertical plate in porous medium in conjunction with thermal radiation. **Open Physics**, 20(1), 302–312.
6. Prashanth, M., & Srinivasa Rao, V. (2025). The effects of MHD slip flow on heat and mass transfer by radiation, chemical reaction, and suction/injection over a shrinking sheet in a porous medium using the Keller Box method. **Heat Transfer**.
7. Jeelani, M. B., & Abbas, A. (2025). Thermal transport in MHD Maxwell hybrid nanofluid flow over inclined stretching porous sheet with effects of chemical reaction, solar radiation and porous medium. **Case Studies in Thermal Engineering**.
8. Swain, B. K. (2021/2024). Effect of second-order chemical reaction on MHD free convective radiating flow over an impulsively started vertical plate. **Journal of Numerical Mathematics and Applications**.
9. Wang, S., et al. (2022). MHD flow, radiation heat and mass transfer of fractional Burgers' fluid in porous medium with chemical reaction. **Computers & Mathematics with Applications**, 115, 68–79.
10. Bejan, A. (2013). **Convection Heat Transfer** (4th ed.). Wiley.
11. Nield, D. A., & Bejan, A. (2017). **Convection in Porous Media** (5th ed.). Springer.
12. Incropera, F. P., DeWitt, D. P., Bergman, T. L., & Lavine, A. S. (2018). **Fundamentals of Heat and Mass Transfer** (8th ed.). Wiley.

13. Cussler, E. L. (2009). **Diffusion: Mass Transfer in Fluid Systems** (3rd ed.). Cambridge University Press.
14. Bird, R. B., Stewart, W. E., & Lightfoot, E. N. (2007). **Transport Phenomena** (2nd ed.). Wiley.
15. Patankar, S. V. (1980). **Numerical Heat Transfer and Fluid Flow**. Hemisphere.
16. Morton, K. W., & Mayers, D. F. (2005). **Numerical Solution of Partial Differential Equations** (2nd ed.). Cambridge University Press.
17. Smith, G. D. (1985). **Numerical Solution of Partial Differential Equations: Finite Difference Methods** (3rd ed.). Oxford University Press.
18. Ames, W. F. (1992). **Numerical Methods for Partial Differential Equations**. Academic Press.
19. Anderson, J. D. (1995). **Computational Fluid Dynamics: The Basics with Applications**. McGraw-Hill.
20. White, F. M. (2016). **Viscous Fluid Flow** (3rd ed.). McGraw-Hill.
21. Schlichting, H., & Gersten, K. (2017). **Boundary-Layer Theory** (9th ed.). Springer.
22. Özisik, M. N. (1993). **Heat Conduction** (2nd ed.). Wiley.
23. Carslaw, H. S., & Jaeger, J. C. (1986). **Conduction of Heat in Solids** (2nd ed.). Oxford University Press.
24. Crank, J. (1975). **The Mathematics of Diffusion** (2nd ed.). Oxford University Press.
25. Crank, J., & Nicolson, P. (1947). A practical method for numerical evaluation of solutions of partial differential equations of the heat-conduction type. **Proceedings of the Cambridge Philosophical Society**, 43, 50–67.
26. Shercliff, J. A. (1965). **A Textbook of Magnetohydrodynamics**. Pergamon Press.
27. Cowling, T. G. (1976). **Magnetohydrodynamics**. Adam Hilger.
28. Sparrow, E. M., & Cess, R. D. (1978). **Radiation Heat Transfer**. Hemisphere Publishing.
29. Eckert, E. R. G., & Drake, R. M. (1972). **Analysis of Heat and Mass Transfer**. McGraw-Hill.
30. Arpaci, V. S. (1966). **Conduction Heat Transfer**. Addison-Wesley.